Defect structures in $LiNbO_3$

1995 J. Phys.: Condens. Matter 7 3627

(http://iopscience.iop.org/0953-8984/7/18/025)

J. Phys.: Condens. Matter 7 (1995) 3627–3635. Printed in the UK

Defect structures in $LiNbO_3$

Y Watanabe†, T Sota†‡, K Suzuki†§, N Iyi‖, K Kitamura‖ and S Kimura‖

† Department of Electrical Engineering, Waseda University, Shinjuku, Tokyo 169, Japan

‡ Advanced Research Center for Science and Engineering, Waseda University, Shinjuku, Tokyo 169, Japan

§ Kagami Memorial Laboratory for Material Science and Technology, Waseda University, Shinjuku, Tokyo 169, Japan

‖ National Institute for Research in Inorganic Materials, Namiki 1-1, Tsukuba-shi, Ibaraki 305, Japan

Received 12 December 1994, in final form 2 February 1995

Abstract. We have re-examined the infrared absorption bands due to the O–H bond-stretching vibration and the polarization characteristics in undoped and MgO-doped $LiNbO_3$ using well-characterized crystals. It has been found that the O–H bond stretching vibrational frequency ν(OH) has a strong correlation with Nb concentration in the crystals. We have also determined the position where hydrogen enters using Novak's empirical relationship between the values of ν(OH) and the length of the hydrogen bond and the structure analysis data for the undoped crystals. On the basis of those results and the polarization characteristics, we have examined the intrinsic and the extrinsic defect structure models in $LiNbO_3$. It has been clarified that the behaviour of ν(OH) reflects the defect structures. The behaviour of ν(OH) supports the Li-site vacancy model as the intrinsic defect structure model, and the corresponding extrinsic defect model. A brief discussion is also given of the behaviour of ν(OH) in crystals simultaneously doped with two kinds of impurity.

1. Introduction

Lithium niobate ($LiNbO_3$) single crystals have a great potential as non-linear optical devices. The light-induced change in the refractive index is the basis of hologram recording and optical conjugation in $LiNbO_3$ but the same photorefractive effect leads to low optical damage resistance, which is a disadvantage in applications such as Q-switch and SHG devices. Anghert *et al* [1] have reported that the optical damage resistance of undoped $LiNbO_3$ increases as the [Li]/[Nb] ratio in the crystals decreases, where [X] denotes the concentration of X. Furukawa *et al* [2] have recently reconfirmed this. It is also well known that the MgO doping at a concentration over 4.5–5.0 mol% reduces the optical damage [3]. Yamamoto *et al* [4] have shown that the optical damage of 1 mol% Sc_2O_3-doped $LiNbO_3$ is approximately half that in undoped $LiNbO_3$ as a function of laser irradiation time [4]. It has also been reported that the inclusion of hydrogen in a high concentration suppresses optical damage [3].

Hydrogen enters the crystals during the growth processes performed in air or during the poling treatment at elevated temperatures in humid atmospheres. The hydrogen in the crystals forms the hydrogen bond O–H···O. In undoped $LiNbO_3$ the following has been shown [5–8]. The O–H bond-stretching vibration causes the infrared absorption band near 3485 cm^{-1}. The corresponding absorption is polarized perpendicular to the c axis. Although the band shape is dependent on the [Li]/[Nb] ratio, no significant change in the peak position is observed. In the case of MgO-doped $LiNbO_3$ [9–13], it has been shown that the shift in

0953-8984/95/183627+09$19.50

ν(OH), the frequency of the O–H bond-stretching vibration, to the higher-frequency region around about 3550 cm^{-1} occurs when the concentration of MgO exceeds 4.5–5.0 mol% depending on the [Li]/[Nb] ratio. Although the threshold concentration seems to coincide with the critical concentration, over which the optical damage resistance is sufficiently high, details are not known. To our best knowledge, no systematic study has been reported for Sc_2O_3-doped $LiNbO_3$. A study on the infrared absorption bands in $LiNbO_3$:Mg, M^{3+} ($M \equiv$ Cr, Nd, Ti, Mn, In, Gd, Er, Tm, Sc, Y or Lu) has been reported by Kovács *et al* [14–16].

As mentioned before, intrinsic and extrinsic defects due to the non-stoichiometry affect considerably the optical damage of the crystals. $LiNbO_3$ itself shows a large variation in the [Li]/[Nb] ratio. So far some intrinsic defect models have been proposed. One is the oxygen vacancy model and the others are cation substitution models. The oxygen vacancy model cannot explain the dependence of the density on the [Li]/[Nb] ratio and, thus, is excluded. For the cation substitution models, there exist two models, namely the Li-site vacancy model and the Nb-site vacancy model. The former, in which the formula is given by $[Li_{1-5x}Nb_x\square_{4x}][Nb]O_3$ where $\square$ denotes the vacancy, has been suggested by Lerner *et al* [17] and recently supported by Iyi *et al* [18]. The latter, in which the formula is given by $[Li_{1-5x}Nb_{5x}][Nb_{1-4x}\square_{4x}]O_3$, has been proposed by Peterson and Carnevale [19] on the basis of a NMR study and supported by Abrahams and Marsh [20] on the basis of an analysis of single-crystal X-ray diffraction patterns. However, it seems that a definite consensus on the intrinsic defect model has not been achieved.

In this paper we have considered the intrinsic defect model in $LiNbO_3$ and also the extrinsic defect model in MgO-doped $LiNbO_3$ based on the behaviour of ν(OH). We have measured ν(OH) in undoped and MgO-doped crystals using well characterized samples. The following has been found. The values of ν(OH) have a strong correlation with [Nb] in the crystals and reflect the intrinsic and the extrinsic defect structures. The behaviour of ν(OH) supports the Li-site vacancy model as the intrinsic defect model, and the corresponding extrinsic defect model in the MgO-doped crystals.

2. Experimental details

Single crystals of undoped $LiNbO_3$ with nearly stoichiometric (sample ST), congruent (sample CG) and highly Li-deficient (sample HN) compositions were prepared. Sample CG was grown by the Czochralski method. The other two samples HN and ST were grown by the floating-zone method and the double-crucible Czochralski method [21], respectively. Detailed conditions of the growth and characteristics of those three samples have been given in [18, 21]. We give only the chemical formulae for the samples in table 1.

Five single crystals of $LiNbO_3$ with different MgO concentrations were also prepared. Samples MG01, MG03, MG05 and MG07 were supplied by the Magnetic and Electronic Materials Research Laboratory, Hitachi Metals, Ltd, and sample MGW5 by the Department of Applied Chemistry, Waseda University. All samples were grown by the Czochralski method.

Chemical analysis for the MgO-doped crystals was conducted as follows. The crushed samples were dissolved in HNO_3–HF solution in a closed Teflon vessel at 150 °C overnight. After filtering to separate the precipitated MgF_2, the resulting solution was passed through an anion exchanger for further separation of Li and Nb ions. The Li and Mg contents were analysed by inductively coupled plasma atomic spectrometry. Nb ions eliminated from the resin by HCl–HF solution were precipitated by cupferron, and the precipitate was dried and incinerated. Weighing of the Nb_2O_5 yielded gave the Nb content. The chemical formulae

Table 1. Chemical formulae of the crystals used in this work.

Sample	Chemical formulae[a]
ST	$Li_{0.994}Nb_{1.0013}\square_{0.004}O_{3.00}$ [b]
CG	$Li_{0.951}Nb_{1.0098}\square_{0.039}O_{3.00}$ [b]
HN	$Li_{0.904}Nb_{1.0192}\square_{0.077}O_{3.00}$ [b]
MG01	$Li_{0.949}Mg_{0.0074}\square_{0.036}Nb_{1.008}O_{3.00}$ [c]
MG03	$Li_{0.924}Mg_{0.032}\square_{0.041}Nb_{1.003}O_{3.00}$ [c]
MG05	$Li_{0.896}Mg_{0.045}\square_{0.056}Nb_{1.003}O_{3.00}$ [c]
MG07	$Li_{0.872}Mg_{0.071}\square_{0.060}Nb_{0.997}O_{3.00}$ [c]
MGW5	$Li_{0.9197}Mg_{0.0434}\square_{0.0382}Nb_{0.9987}O_{3.00}$

[a] $\square$ denotes a vacancy.

[b] For chemical formulae obtained by x-ray refinement, see table VII in [18].

[c] For the lattice constants and the density of these samples, see [26].

obtained are given in table 1. Note that a structure analysis has not been performed for samples MG01, MG03, MG05, MG07 and MGW5.

The infrared transmittance and reflectance were recorded with a Hitachi I-3000 grating spectrometer in the range from 3400 to 3600 cm^{-1} at room temperature. The spectral resolution was 2.0 ± 0.5 cm^{-1}. The absorption coefficient were calculated taking account of multiple reflection. For polarization measurements a wire grid polarizer was used. In this case, only the transmittance for each sample was measured to save time.

3. Results

We first give the results of experiments using unpolarized light. Figure 1(*a*) shows the absorption coefficients of samples ST, CG and HN. It should be noted that poling treatment had been performed on sample CG. As is known [5–8], the shape of the absorption coefficient depends on the [Li]/[Nb] ratio, but no significant change in ν(OH) was observed. Our results reconfirmed this. The absorption coefficients of the MgO-doped crystals are shown in figure 1(*b*) where that of sample CG is also shown for comparison. The shapes of the absorption coefficient for the MgO-doped crystals are similar to that for sample CG. The shift in ν(OH) to a higher frequency occurs only for samples MG07 and MGW5. The origins of the small peaks at approximately 3580 and 3592 cm^{-1} for sample MGW5 are not known and therefore we shall not discuss them throughout this paper.

To estimate the values of ν(OH) causing the infrared absorption and the corresponding OH concentration n_{OH}, we have decomposed the absorption spectra into some spectra using the Lorentzian or the Gaussian lineshape functions where ν(OH), the intensity I and the half-width Γ at half-maximum have been treated as fitting parameters. The values obtained for ν(OH), I and Γ are listed in table 2. n_{OH} corresponding to each decomposed spectrum has been calculated using the formula given by Klauer *et al* [22]. The values calculated for n_{OH} are listed in table 2. It is found from table 2 that n_{OH} is at most of the order of 10^{18} cm^{-3} and the concentration is much smaller than the intrinsic defect density in the crystals.

In figure 2 is shown the dependence of ν(OH) on [Nb] in the crystals. The following is found. While the values of ν(OH) in the crystals with [Nb]/[$LiNbO_3$] > 1 or [Nb]/[$LiNbO_3$ + MgO] > 1 lie in the region 3460–3500 cm^{-1}, those of ν(OH) in the crystals with [Nb]/[$LiNbO_3$ + MgO] < 1 lie in the range 3525–3550 cm^{-1}. It is worthwhile mentioning that the values of ν(OH) are mainly affected by [Nb] in the crystals (compare sample MGW5 with sample MG05). Note that the essential features in figure 2 do not depend on the spectrum decomposition method.

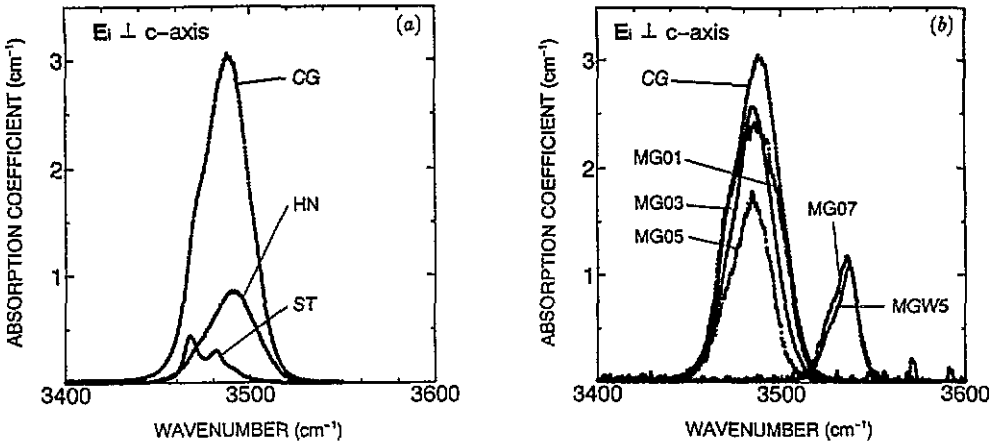

Figure 1. Dependences of the absorption coefficients due to the O–H bond stretching vibration on the frequencies ν(OH) in (*a*) un-doped crystals and (*b*) MgO-doped crystals. For the chemical formulae of samples, see table 1.

Next we describe the results of polarization measurements. In figure 3 are plotted the integrated absorption intensities estimated from the transmittance alone as a function of the angle θ formed by the c axis and the electric field vector of the light propagating perpendicular to the c axis. The data obtained for the undoped crystals fit excellently to the expected function $\sin^2\theta$ [13]. It has been reconfirmed that the O–H bonds lie in the plane perpendicular to the c axis. For the MgO-doped crystals, the deviation from the function $\sin^2\theta$ becomes marked at $\theta \simeq 0$ and $\theta \simeq \pi$ for both sample MGW5 and sample MG07. The deviation indicates that the angle φ between the direction of the O–H bonds and the plane perpendicular to the c axis takes a finite value. To estimate φ, we have used the equation given by Kovács *et al* [13]. The maximum φ value of 16° has been obtained for sample MGW5. When the uncertainty in measurements is taken into account, the accuracy of φ is better than ±2.5°.

4. Discussion

We consider the position where the hydrogen bonds are formed in the undoped crystals. The empirical relationship between ν(OH) and R(O···O) and/or r(O–H) has been given by Novak [23], where R(O···O) and r(O–H) denote the hydrogen bond length and the bond length between an oxygen ion and a proton in the hydrogen bond, respectively. Using this relation as a guide we have estimated R(O···O) and r(O–H) for each ν(OH). The results are given in table 2. The values of R(O···O) for the samples ST, CG and HN are 2.86 ± 0.02 Å. Here we should comment on the use of Novak's empirical relationship. There is, unfortunately, no guarantee whether it can be applied to $LiNbO_3$ or not. However, we believe that its use may be justified for the following reasons.

(i) The values of ν(OH) and ν(OD) [24] in $LiNbO_3$, where ν(OD) is the oxygen–deuteron (D) bond-stretching vibrational frequency in deuterated samples, lead to $\nu(OH)/\nu(OD) = 1.356$, which means that the weak hydrogen bond, and the correlation between the ratio $\nu(OH)/\nu(OD)$ and ν(OH) are just the same as predicted from figure 11 in Novak's [23] paper.

(ii) The values of R(O···O) estimated from the empirical relationship are not different significantly from those speculated previous [5, 8].

Table 2. Values of the O–H bond-stretching vibrational frequencies ν(OH), the intensity I and the half-width Γ at half-maximum for each decomposed absorption spectrum. Estimated values of the concentration n_{OH}, of hydrogen, the bond length $R(O\cdots O)$ between oxygen ions, and the O–H bond length r(O–H) for each decomposed absorption spectrum are also given.

Sample	ν(OH) (cm^{-1})	Γ (cm^{-1})	I (cm^{-2})	n_{OH} [22] (cm^{-3})	$R(O\cdots O)$ [23] (Å)	r(O–H) [23] (Å)
ST	3460.5	5.0	0.7592	3.793×10^{16}	2.8456	0.9896
	3467.6	3.6	2.7591	1.378×10^{17}	2.8527	0.9890
	3474.3	4.4	2.2347	1.161×10^{17}	2.8596	0.9884
	3481.8	4.0	1.8451	9.214×10^{16}	2.8678	0.9878
	3490.3	5.5	1.9583	9.977×10^{16}	2.8775	0.9870
CG	3469.5	7.0	17.0431	8.514×10^{17}	2.8546	0.9888
	3488.4	13.5	84.6411	4.225×10^{18}	2.8753	0.9872
HN	3470.0	9.0	4.1563	2.076×10^{17}	2.8551	0.9888
	3491.5	14.0	24.5892	1.228×10^{18}	2.8789	0.9869
MG01	3467.4	6.1	12.7758	6.382×10^{17}	2.8525	0.9890
	3476.5	9.7	22.7157	1.134×10^{18}	2.8620	0.9882
	3491.7	12.3	52.5900	2.626×10^{18}	2.8791	0.9869
MG03	3468.2	6.8	12.5613	6.274×10^{17}	2.8533	0.9889
	3485.2	10.9	56.3117	2.812×10^{18}	2.8716	0.9875
	3500.7	10.1	5.2179	2.604×10^{17}	2.8900	0.9861
MG05	3469.4	9.3	10.0975	5.043×10^{17}	2.8545	0.9888
	3485.7	10.6	36.5581	1.825×10^{18}	2.8722	0.9874
MG07	3526.6	5.9	10.3798	5.177×10^{17}	2.9250	0.9839
	3536.5	5.6	11.8267	5.897×10^{17}	2.9399	0.9830
	3546.2	2.6	0.9802	4.886×10^{16}	2.9554	0.9822
MGW5	3528.3	7.0	6.5571	3.270×10^{17}	2.9275	0.9837
	3536.7	5.1	4.7586	2.372×10^{17}	2.9402	0.9830
	3538.6	5.2	7.1441	5.563×10^{17}	2.9432	0.9829

Taking account of the polarization characteristics, we consider the oxygen plane perpendicular to the c axis. The oxygen plane is schematically illustrated in figure 4. The values of $R(O\cdots O)$ in figure 4 correspond to those for the sample ST [18]. It is found that the values of $R(O\cdots O)$ in the oxygen triangle just above Nb_{Nb}^{5+}, where Nb_{Nb}^{5+} denotes Nb^{5+} at the Nb site, is 2.870 Å and those of $R(O\cdots O)$ in the other triangles are very much different from the value of 2.86 ± 0.02 Å estimated from ν(OH). Therefore, it is natural to consider that hydrogen enters the oxygen triangles just above Nb_{Nb}^{5+}. The structure analysis in [18] indicates that the values of $R(O\cdots O)$ in the oxygen triangles are 2.870 Å, 2.871 Å and 2.869 Å for the samples ST, CG and HN. This behaviour of $R(O\cdots O)$ is consistent with that of ν(OH). Note that the values of the position parameters obtained in the structure analysis are averaged.

We discuss the intrinsic defect structure on the basis of the behaviour of ν(OH), the polarization characteristics and the position of hydrogen. There is no vacancy at the Nb site in the Li-site vacancy model. On the other hand the Nb-site vacancy model predicts that the amount of Nb_{Nb}^{5+} decreases and that of the vacancy increases as the [Li]/[Nb] ratio decreases. Here let us recall the experimental results: firstly no significant change in ν(OH), secondly a slight dependence of the absorption band change on the [Li]/[Nb] ratio, and thirdly the

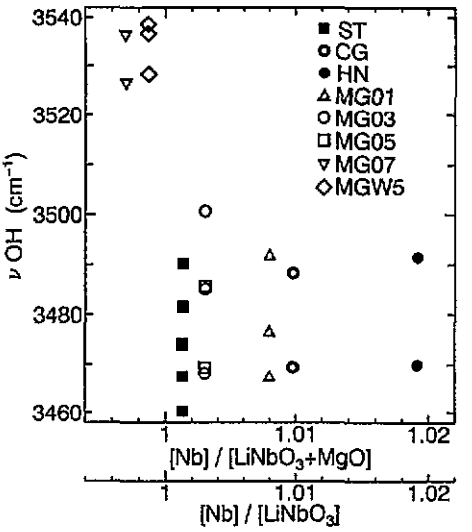

Figure 2. Dependences of the O–H bond stretching vibrational frequencies ν(OH) for each decomposed spectrum given in table 2 on [Nb] in the crystals. For the chemical formulae of samples, see table 1.

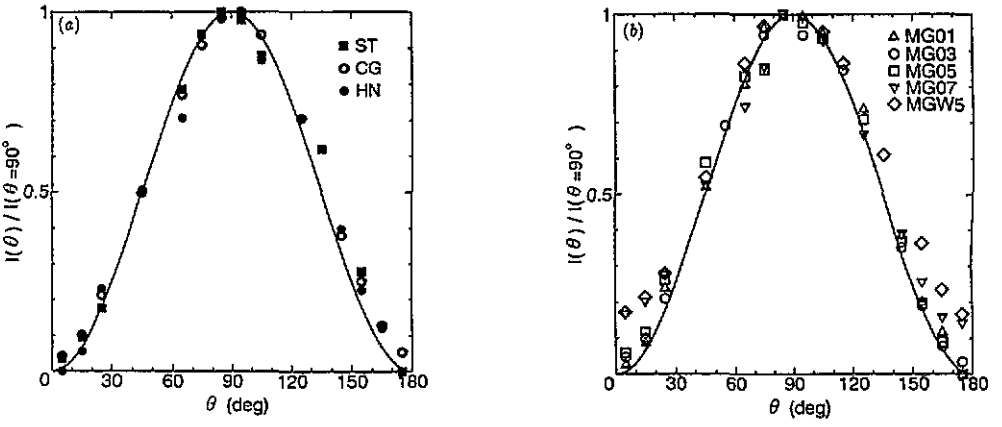

Figure 3. Polarization dependences of integrated absorption intensities estimated from the transmittance spectra for (*a*) undoped crystals and (*b*) MgO-doped crystals, where we define θ as the angle formed by the *c* axis and the electric field vector of the light propagating perpendicular to the *c* axis. For the chemical formulae of samples, see table 1.

O–H bond lying in the oxygen plane perpendicular to the *c* axis. The Li-site vacancy model naturally explains the first and the third results from the viewpoint of no vacancy at the Nb site in the ideal crystal. Note that the distortion of the oxygen octahedron around the Nb^{5+} is dominated not by the change in the Li-site charge but by that of the Nb-site charge. The second result may be attributed to the fluctuation in $R(O\cdots O)$ or in r(O–H) in the oxygen triangle where hydrogen enters into the real crystals. The Nb-site vacancy model also explains the first result because the oxygen triangle just above $\square_{Nb}$ is the preferred site for hydrogen and n_{OH} is much smaller than the intrinsic defect density in all undoped crystals. The second result may also be attributed to the fluctuation in $R(O\cdots O)$ of in r(O–H) as in the case of the Li-site vacancy model. However, the third result and the distorted oxygen

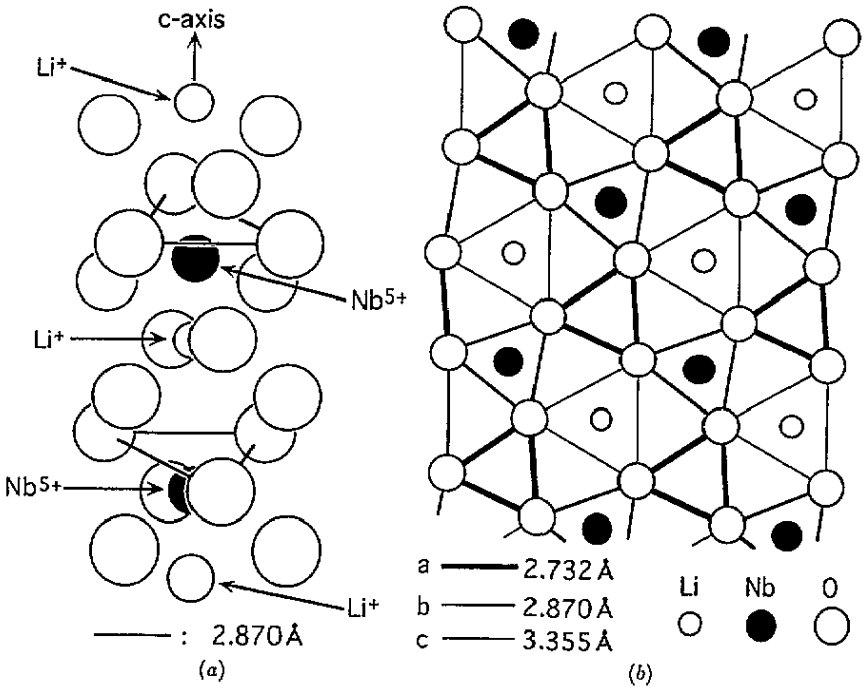

Figure 4. Schematic illustration of (*a*) the crystal structure in $LiNbO_3$ and (*b*) the oxygen plane just above Nb^{5+}. The values of the bond length given in figure are calculated from the structure analysis data for the nearly stoichiometric crystal. For the details of the structure analysis data, see [18]. Note that, in (*b*), Nb^{5+} and Li^+ are located, below and above the oxygen plane, respectively.

triangle or the change in the O–H bond direction expected from the Nb-site vacancy model contradict each other. Therefore, the Nb-site vacancy model is probably not appropriate as the intrinsic defect structure model. Our interpretation is consistent with the results of computer simulation on the defect formation energy in $LiNbO_3$ performed by Donnerberg *et al* [25].

We show that the experimental results for the MgO-doped crystals also contradict the extrinsic defect structure model based on the Nb-site defect model proposed by Grabmaier *et al* [26]. According to them, Mg^{2+} substitutes for Nb_{Li}^{5+} up to a Mg content of 3.0 mol% and then for Li_{Li}^{+} up to a Mg content of 8.0 mol%, leaving the vacancies at the Nb site, which vanish at a Mg concentration of 8.0 mol%. When the Mg content exceeds 8.0 mol%, Mg^{2+} substitute for Nb_{Nb}^{5+}, leaving the vacancies at the Li site. Here the following should be mentioned. We measure the Mg content by the percentage $[MgO]/[LiNbO_3 + MgO]$ ratio throughout this paper but Grabmaier *et al* use the $[Mg]/[Li + Nb + Mg + \square]$ ratio in their original paper. The results of the chemical analysis given in table 1 can be consistently plotted on figure 2 of the paper by Grabmaier *et al* [26] taking account of the above. It follows from their model that both the values of ν(OH) and the polarization characteristics hardly change up to a Mg content of 8.0 mol%. This is because the vacancies remain at the Nb site (see the previous paragraph). Thus their model cannot explain the shift in ν(OH) for samples MG07 and MGW5. Therefore it seems that the Nb-site vacancy model should be excluded as the intrinsic defect model and also the extrinsic defect structure model based on it.

We consider the extrinsic defect structure model based on the Li-site vacancy model. Figure 2 shows that, when $[Nb]/[LiNbO_3 + MgO] > 1$, the ν(OH) values for the MgO-doped crystals are almost the same as for sample CG. The experimental results mean that $R(O\cdots O)$ and r(O–H) in the oxygen triangle do not significantly change, and the Nb site is hardly disturbed. Thus it follows that doped Mg^{2+} does not enter the Nb site but does enter the Li site, and all vacancies needed to satisfy charge neutrality remain at the Li site. The fact that there is not appreciable deviation of the polarization data from the expected function also supports this interpretation. Furthermore it is apparent from figure 2 that doped Mg^{2+} pushes out Nb^{5+} from the Li site. When the relation $[Nb]/[LiNbO_3 + MgO] < 1$ holds, a shift in ν(OH) occurs and the polarization characteristics change considerably. The condition $[Nb]/[LiNbO_3 + MgO] < 1$ indicates the situation that all Nb_{Li}^{5+} and some Nb_{Nb}^{5+} are pushed out. In this case there is only the possibility that Mg^{2+} substitute for Nb_{Nb}^{5+} owing to the charge neutrality condition. The change in charge at the Nb site and the difference between the ionic radii in octahedral coordination due to the exchange of Mg^{2+} and Nb_{Nb}^{5+} may cause the change in the O–H bond length and direction, i.e. making $R(O\cdots O)$ longer and/or r(O–H) shorter and φ finite. Thus the shift in ν(OH) and the change in the polarization characteristics can be attributed to the exchange of Mg^{2+} and Nb_{Nb}^{5+}. Unfortunately we have no data on the structure analysis for the MgO-doped crystals. It is desirable to perform a structure analysis to confirm the above-mentioned interpretation. Note that our scenario with respect to the extrinsic defect structure model in MgO-doped $LiNbO_3$ is consistent with the quite recent results of Iyi *et al* [27] and those of a Monte Carlo simulation of channelling phenomena in $LiNbO_3$ performed by Rebouta *et al* [28].

We explain the absorption bands with a definite double-peak structure due to ν(OH) in $LiNbO_3$:Mg^{2+}, M^{3+} crystals [14–16] within our scenario derived above. In such crystals the amount of Mg^{2+} is sufficient to push out Nb_{Li}^{5+}, and some Mg^{2+} is considered to substitute for Nb_{Nb}^{5+}, too. Let us assume that the codoped M^{3+} also substitute for Nb_{Nb}^{5+} and $n_{OH} < [Mg_{Nb}^{2+}] + [M_{Nb}^{3+}]$. If this is the case, two kinds of distorted oxygen octahedron around X_{Nb} where $X \equiv Mg^{2+}$ or M^{3+} exist. The oxygen triangle just above X_{Nb}, which is a part of the distorted oxygen octahedron, is apparently the preferred position for hydrogen. It is natural that the values of $R(O\cdots O)$ or r(O–H) in the oxygen triangles are different depending on the values of ionic charges and/or those of ionic radius. As a result two kinds of ν(OH) exist: one is due to the O–H bond in the oxygen triangle just above Mg_{Nb}^{2+} and the other is due to that just above M_{Nb}^{3+}. Thus it is not surprising that absorption bands with a definite double-peak structure appear. The difference between the ν(OH)-values is mainly attributed to the difference between the charges Mg^{2+} and M^{3+}, causing a difference between the electrostatic forces. When the condition $n_{OH} > [Mg_{Nb}^{2+}] + [M_{Nb}^{3+}]$ is satisfied, it is expected that absorption bands with a definite triple-peak structure will appear. In this case the position of the third peak is the same as that of ν(OH) in undoped crystals. If all M^{3+} substitute for the Li site and $n_{OH} > [Mg_{Nb}^{2+}]$, the absorption bands are expected to have a definite double-peak structure. The position of one peak is almost the same as that of ν(OH) in undoped crystals, and the position of the other peak is the same as that of ν(OH) in MgO-doped crystals. Similar considerations can be applied to the case of absorption bands with a definite double-peak structure in crystals doped with only one kind of impurity, e.g. $LiNbO_3$:Mg^{2+} [9, 10]. Note that in any case the fluctuation in $R(O\cdots O)$ or r(O–H) causes minor structures in the absorption bands.

Here we would like to make a few comments on the behaviour of ν(OH) in Sc_2O_3-doped crystals. From our discussion, it is possible to observe the shift in ν(OH) to the higher-frequency region in Sc_2O_3-doped crystals under the condition that Sc^{3+} substitute for Nb_{Nb}^{5+}. It is also expected from the difference between the charges of Sc^{3+} and Mg^{2+}

that the concentration of Sc where the shift in ν(OH) is observed is different from that of MgO and the amount of the frequency shift is smaller than in MgO-doped crystals. A study of the behaviour of ν(OH) in Sc_2O_3-doped crystals would confirm our interpretation.

In summary we have discussed the defect structure model in $LiNbO_3$ based on the behaviour of ν(OH) obtained experimentally. We have found that the values of ν(OH) have a strong correlation with [Nb] in the crystals and that the behaviour of ν(OH) reflects the intrinsic and the extrinsic defect structures. The behaviour of ν(OH) supports the Li-site vacancy model as the intrinsic defect structure model, and the corresponding extrinsic defect structure model.

Acknowledgments

We would like to thank Professor A Hirata, Department of Applied Chemistry, Waseda University and Dr Y Furukawa and Dr M Sato, Magnetic and Electronic Materials Research Laboratory, Hitachi Metals Ltd for supplying samples doped with MgO. We are also grateful to Mr S Shimamura for his assistance in experiments.

References

[1] Anghert N B, Pashkov V A and Solov'yeva N M 1972 *Zh. Eksp. Teor. Fiz.* **26** 1666
[2] Furukawa Y, Sato M, Kitamura K, Yajima Y and Minakata M 1992 *J. Appl. Phys.* **72** 3250
[3] For a review article, see Schirmer O F, Thiemann O and Wöhlecke M 1991 *J. Phys. Chem. Solids* **52** 185
[4] Yamamoto J K, Kitamura K, Iyi N, Kimura S, Furukawa Y and Sato M 1992 *Appl. Phys. Lett.* **61** 2156
[5] Herrington J R, Dischler B, Räuber A and Schneider J 1973 *Solid State Commun.* **12** 351
[6] Kovács L, Szalay V and Capelletti R 1984 *Solid State Commun.* **52** 1029
[7] Feng Xi-qi, Shao Tian-hao and Zhang Ji-zhou 1991 *J. Phys.: Condens. Matter* **3** 4145
[8] Kovács L, Wöhlecke M, Jovanovič A, Polgár K and Kapphan S 1991 *J. Phys. Chem. Solids* **52** 797
[9] Bryan D A, Gerson R and Tomashke H E 1984 *Appl. Phys. Lett.* **44** 847
[10] Bryan D A, Rice R R, Gerson R, Tomaschke H E, Sweeney K L and Halliburton L E 1985 *Opt. Eng.* **24** 138
[11] de Rosendo Ma J, Arizmendi L, Cabrera J M and Agulló-López F 1986 *Solid State Commun.* **59** 499
[12] Polgár K, Kovács L, Földvári I and Cravero I 1986 *Solid State Commun.* **59** 375
[13] Kovács L, Polgár K and Capelletti R 1987 *Cryst. Latt. Defects Amorph. Matter.* **15** 115
[14] Kovács L, Földvári I, Cravero I and Polgár K 1988 *Phys. Lett.* **133A** 433
[15] Kovács L, Szaller Zs, Cravero I, Földvári I and Zaldo C 1990 *J. Phys. Chem. Solids* **51** 417
[16] Kovács L, Rebouta L, Soares J C, da Dilva M F, Hage-Ali M, Stoquert J P, Siffert P, Sanz-Garcia J A, Corradi G, Szaller Zs and Polgár K 1993 *J. Phys.: Condens. Matter* **5** 781
[17] Lerner P, Legras C and Dumas J P 1968 *J. Cryst. Growth* **3–4** 231
[18] Iyi N, Kitamura K, Izumi F, Yamamoto J K, Hayashi T, Asano H and Kimura S 1992 *J. Solid State Chem.* **101** 340
[19] Peterson G E and Carnevale A 1972 *J. Chem. Phys.* **56** 4848
[20] Abrahams S C and Marsh P 1986 *Acta Crystallogr.* B **42** 61
[21] Kitamura K, Yamamoto J K, Iyi N, Kimura S and Hayashi T 1992 *J. Cryst. Growth* **116** 327
[22] Klauer S, Wöchlecke M and Kapphan S 1992 *Phys. Rev.* B **45** 2786
[23] Novak A 1974 *Struct. Bonding* **18** 177
[24] Förster A, Kapphan S and Wöhlecke M 1987 *Phys. Status Solidi* b **143** 755
[25] Donnerberg H, Tomlinson S M, Catlow C R A and Schirmer O F 1989 *Phys. Rev.* B **40** 11909
[26] Grabmaier B C, Wersing W and Koestler W 1991 *J. Cryst. Growth* **110** 339
[27] Iyi N, Kitamura K, Yajima Y, Kimura S, Furukawa Y and Sato M 1995 *J. Solid State Chem.* at press
[28] Rebouta L, Smulders P J M, Boerma D O, Agulló-López F, da Silva M F and Soares J C 1993 *Phys. Rev.* B **48** 3600